

Drift of spiral waves controlled by a polarized electric field

Jiang-Xing Chen, Hong Zhang,^{a)} and You-Quan Li

Zhejiang Institute of Modern Physics and Department of Physics, Zhejiang University, Hangzhou 310027, China

(Received 19 September 2005; accepted 2 November 2005; published online 5 January 2006)

The drift behavior of spiral waves under the influence of a polarized electric field is investigated in the light that both the polarized electric field and the spiral waves possess rotation symmetry. Numerical simulations of a reaction-diffusion model show that the drift velocity of the spiral tip can be controlled by changing the polarization mode of the polarized electric field and some interesting drift phenomena are observed. When the electric field is circularly polarized and its rotation follows that of the spiral, the drift speed of the spiral tip reaches its maximal value. On the contrary, opposite rotation between the spiral and electric field locks the drift of the spiral tip. Analytical results based on the weak deformation approximation are consistent with the numerical results. We hope that our theoretical results will be observed in experiments, such as the Belousov-Zhabotinsky reaction. © 2006 American Institute of Physics. [DOI: 10.1063/1.2145754]

Numerous chemical and biological systems can be classified as excitable media. Sufficiently strong perturbations in such media can excite self-sustained nonlinear propagating waves that can form rotating vortexlike patterns, spiral waves in two dimensions, or scroll waves in three dimensions.^{1,2} They are probably the most frequently encountered self-organizing structures in excitable media observed in many different systems, such as the prototypical Belousov-Zhabotinsky (BZ) reaction,³ catalytic surface processes,⁴ aggregating colonies of social amoebae and other microorganisms,⁵ and propagating patterns of heart tissue excitations.⁶ In particular, they play an essential role in heart diseases such as arrhythmia and fibrillation.⁶⁻⁸ In order to understand or control the dynamics of spiral waves, many methods have been employed to investigate the drift behavior of spiral waves (usually in chemical reaction-diffusion systems), such as periodic illuminations,⁹⁻¹⁷ periodic mechanical deformation,¹⁸ electric field,¹⁹⁻²⁹ etc.

In the presence of a dc electric field, Steinbock *et al.*¹⁹ show that the center of spiral waves in the BZ reaction drifts with a velocity whose two components are parallel and perpendicular to the applied field. The component of the drift perpendicular to the electric field changes its sign with chirality of the spiral wave. In Ref. 28, Munuzuri *et al.* observe that the spiral in the BZ reaction undergoes a directional drift when the frequency of an ac electric field is twice that of the spiral frequency. They found the direction of the spiral drift changes continuously between 0 and 360° when the phase shift between ac electric field and spiral rotation varies from 0 to 180°. In our recent work,²⁹ spiral drift induced by dc and ac electric fields is studied, and an approximate formula of the electric-field-induced drift velocity is derived. With this approximate formula we are able to explain the main features appearing in the directional spiral-tip-drift problems, such as the constant drift of the dc electric

field and the net drift of the ac electric field at $\omega=2\omega_0$, and the phase and chirality relations in these drift processes.

In review of previous works that focus on the influence of electric fields on spiral waves dynamics, the electric field is applied merely in one direction. Since spiral waves rotate around its center possessing rotation symmetry, it will be worthwhile to investigate spiral-drift behavior caused by a polarized electric field that also possesses rotation symmetry (see Fig. 1). In this paper, we will investigate the drift behavior of a spiral under the influence of a polarized electric field. Applying two ac electric fields perpendicular to each other to the system, one can get a polarized electric field. Tuning the phase difference between those two perpendicular fields, one can produce a circular, an elliptical, or a linear polarized electric field. Some interesting drift phenomena of the spiral are observed for the aforementioned different modes of polarization. Analytical results obtained in the weak deformation approximation agree with our numerical results qualitatively.

With an additional term $ME \cdot \nabla u$, a two-variable reaction-diffusion model can describe the propagation of spiral waves in the presence of an external electric field E :

$$\frac{\partial u}{\partial t} = \frac{1}{\epsilon} f(u, v) + D_u \Delta u + ME_x \frac{\partial u}{\partial x} + ME_y \frac{\partial u}{\partial y}, \quad (1)$$

$$\frac{\partial v}{\partial t} = g(u, v) + D_v \Delta v,$$

where the variables u and v can be interpreted as the concentrations of the reagents, etc., and $1/\epsilon$ is a parameter characterizing the excitability of the medium. Parameter M is the ion mobility and $E=(E_x, E_y)$ the electric field. For numerical simulations, we will consider a modified FitzHugh-Nagumo model,³⁰ where $D_u=1$ and $D_v=0$, $f(u, v)=-u(u-1)[u-(v+b)/a]$ and $g(u, v)=-v$, if $0 \leq u < 1/3$; $g(u, v)=1-6.75u(u-1)^2-v$, if $1/3 \leq u \leq 1$; and $g(u, v)=1-v$, if $u > 1$. The simulation is performed on a system of 35×35 size with

^{a)}Author to whom correspondence should be addressed. Electronic mail: hzhang@zimp.zju.edu.cn

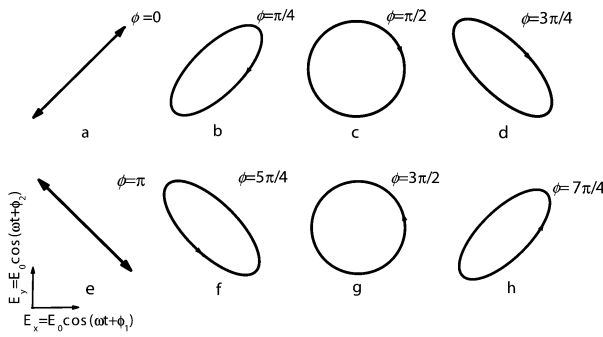


FIG. 1. [(a)–(h)] Polarized electric fields at different phase differences.

no-flux boundary conditions. Discretizations with $\Delta x = \Delta y = 0.175$ and $\Delta t = 0.001$ have been used in an Euler scheme. With suitable parameter values and initial condition, the system will have a dense and rigidly rotating spiral wave solution.

Now we investigate the response of a spiral under the influence of a polarized electric field. The polarized electric field is generated by the following process: two ac electric fields $E_x = E_0 \cos(\omega t + \phi_1)$ and $E_y = E_0 \cos(\omega t + \phi_2)$ are applied along the x and y axes, respectively. Their superposition $\mathbf{E} = (E_x, E_y)$ gives rise to a polarized electric field rotating in two dimensions, which is shown in Fig. 1. The mode of such a polarized electric field is characterized by the phase difference $\phi = \phi_2 - \phi_1$. The electric field is linearly polarized [see Figs. 1(a) and 1(e)] when $\phi = 0$ or π ; it is circularly polarized when $\phi = \pi/2$ or $3\pi/2$, i.e., levorotatory polarization in Fig. 1(c) and dextrorotatory polarization in Fig. 1(g); the modes of electric field in Figs. 1(b), 1(d), 1(f), and 1(h) are of elliptical polarization for $\phi = \pi/4, 3\pi/4, 5\pi/4,$ and $7\pi/4$. In order to simplify the simulation process, we set $\phi_2 = 0$. In the following discussions, we will consider the drift of a spiral under a weak polarized electric field ($ME_0 = 0.02$) with different phase differences.

For a given angular frequency ω of the polarized electric field, the system resonates at frequency $\omega = 2\omega_0$ (ω_0 is the angular frequency of the spiral wave), which results in a spiral drift in a straight line. The corresponding trajectories of the spiral tip under the influence of polarized electric fields are shown in Fig. 2. We first investigate the drift behavior of a counterclockwise rotating spiral wave [see Fig. 2(a), $\sigma = 1$, $\sigma = \pm 1$ represent the chirality of the spiral, $\sigma = +1$ for counterclockwise rotating spiral, while $\sigma = -1$ for the clockwise one]. When the electric field is counterclockwise rotating polarized [phase difference $\phi = 3\pi/2$, see Fig. 1(g)], the drift speed reaches its maximal value. It shows that when the electric field is circularly polarized and its rotation follows that of the spiral wave, the spiral drifts the fastest. As the phase difference is changed to $\phi = \pi/2$ (clockwise circularly polarized), the spiral rotates around the core region but does not drift. In this case, the polarized electric field rotates contrary to that of the spiral. Reversing the direction of the polarized electric field results in a big change of drift velocity; this suggests that the relative rotation direction between the polarized electric field and the spiral closely relates to

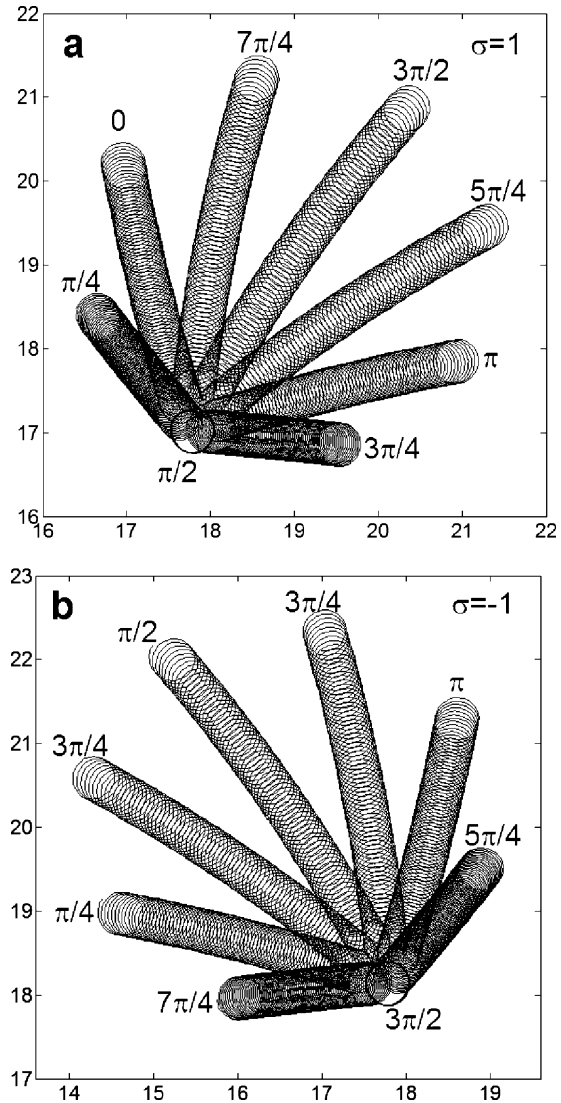


FIG. 2. Dependence of the drift on the phase difference at resonant frequency $\omega = 2\omega_0$ for (a) $\sigma = 1$ and (b) $\sigma = -1$. Parameters in Eq. (1) are $a = 0.84$, $b = 0.07$, and $\varepsilon = 0.02$.

spiral-drift behavior. It shows that the drift velocity can be controlled by changing either the intensity or the phase difference of the polarized electric field.

Figure 2 shows certain symmetry of the spiral tip trajectories. With regard to the trajectory at phase difference $3\pi/2$ in Fig. 2(a), one can see that these trajectories are symmetrical. For example, the drift velocities for $5\pi/4$ and $7\pi/4$ are symmetrical along the drift velocity for $3\pi/2$. In Fig. 3(a), the drift speed dependence on the phase difference is presented. One can see that the drift speed can be changed in practice by varying the phase difference. The symmetry in Fig. 2 is clearly indicated by the speed-phase difference curve [see the vertical dot line in Fig. 3(a)]. The drift direction can also be controlled by changing the phase difference of the polarized electric field, which is shown in Fig. 3(b).

Numerical simulations show that the drift speed does not change when the phase difference is fixed. For example, when we change (ϕ_2, ϕ_1) from $(0, -\pi/3)$ to $(\pi/2, \pi/6)$ or $(3\pi/4, 5\pi/12)$, the drift speed keeps invariant.

In order to investigate the influence of chirality σ on

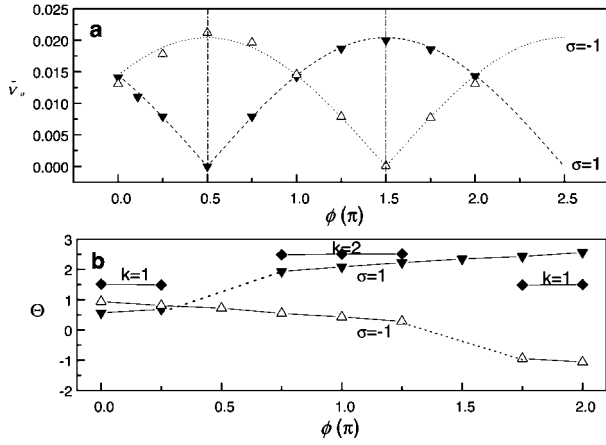


FIG. 3. (a) Numerical (scatter) and theoretical (line) results \bar{V}_d vs ϕ . (b) Drift angle Θ and the sum of that vs phase difference ϕ . When drift velocity is zero, drift angle is neglected: $\phi = \pi/2$ for $\sigma=1$ and $\phi = 3\pi/2$ for $\sigma=-1$.

spiral-drift behavior, let us go back to Fig. 2 (from $\sigma=1$ to $\sigma=-1$). Compared with Fig. 2(a) ($\sigma=1$), trajectories in Fig. 2(b) ($\sigma=-1$) show that the drift velocity for $\sigma=-1$ is different from that for $\sigma=1$. The drift speed for $\sigma=-1$ reaches its maximal value at phase difference $\phi = \pi/2$ and becomes zero at $\phi = 3\pi/2$, which can also be seen in Fig. 3(a). Comparing the result of $\sigma=1$ with that of $\sigma=-1$, one can see that the polarization mode of the electric field and the relative rotation relation between the spiral and the electric field play important roles in spiral drift. The same relative rotation between the spiral and the circular polarized electric field induces spiral drift the fastest, while reversed relative rotation leads to spiral locking. The maximal value for $\sigma=1$ is at $\phi = 3\pi/2$, while it is at $\phi = \pi/2$ for $\sigma=-1$. For $\sigma=-1$, drift angles decrease with phase difference, contrary to that for $\sigma=1$ [Fig. 3(b)]. In addition, at a fixed phase difference, the corresponding sum value of drift angles for $\sigma=1$ and $\sigma=-1$ is equal to $k\pi + \pi/2$, $k=1, 2, \dots$ [Fig. 3(b)]. For example, at phase difference $\phi=0, \pi/4$, and $7\pi/4$, the corresponding sum value of drift angle is $\Theta_{\sigma=1} + \Theta_{\sigma=-1} = 3\pi/2$ ($k=1$); at phase difference $\phi=3\pi/4, \pi$, and $5\pi/4$, $\Theta_{\sigma=1} + \Theta_{\sigma=-1} = 5\pi/2$ ($k=2$).

For $\omega=0$ and $\phi=0$, the system is under control by a direct electric field ($E_x=E_y=E_0$). The drift speed \bar{V}_d linearly increases with the amplitude of the weak dc electric field $E_d = \sqrt{E_x^2 + E_y^2} = \sqrt{2}E_0$, which can be seen in Fig. 4.

In order to attain insight into the underlying mechanism of the spiral-tip-drift behavior, we will make theoretical analysis under the weak deformation approximation.²⁹ Considering the influence of two arbitrary external fields $\Gamma_1(x, y, t)$ and $\Gamma_2(x, y, t)$ on the system, we have

$$\frac{\partial u}{\partial t} = \frac{1}{\epsilon} f(u, v) + D_u \Delta u + \Gamma_1, \quad \frac{\partial v}{\partial t} = g(u, v) + D_v \Delta v + \Gamma_2. \quad (2)$$

For small Γ_1 and Γ_2 , we assume that the deformation of the spiral around the tip is weak, and numerical results show that this approximation is good for a resonantly drifting spiral that was dense and rigidly rotating.^{17,29} In this approximate, we can derive the drift velocity of the spiral tip,²⁹

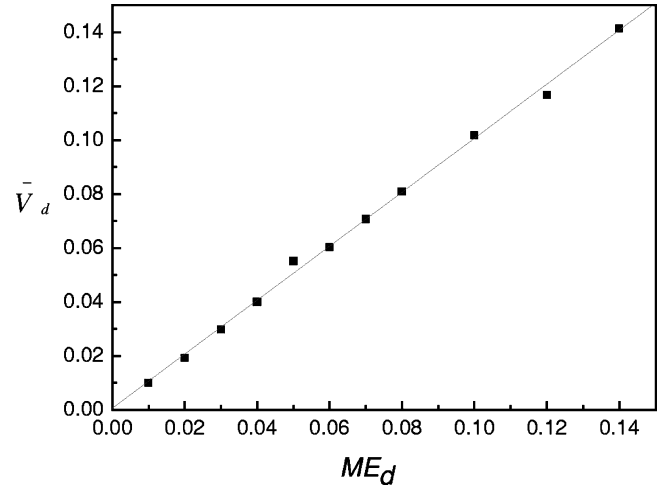


FIG. 4. Drift speed \bar{V}_d vs the strength of constant electric field E_d .

$$V_x(t) = [(-\Gamma_1 \cdot \hat{v}_y + \Gamma_2 \cdot \hat{u}_y) / (\hat{u}_x \hat{v}_y - \hat{u}_y \hat{v}_x)]_{\text{tip}},$$

$$V_y(t) = [(\Gamma_1 \cdot \hat{v}_x - \Gamma_2 \cdot \hat{u}_x) / (\hat{u}_x \hat{v}_y - \hat{u}_y \hat{v}_x)]_{\text{tip}},$$

where $[\hat{u}_x]_{\text{tip}} = a_1 \cos(\omega_0 t - \beta)$, $[\hat{u}_y]_{\text{tip}} = \sigma a_1 \sin(\omega_0 t - \beta)$, $[\hat{v}_x]_{\text{tip}} = a_2 \cos(\omega_0 t - \alpha)$, $[\hat{v}_y]_{\text{tip}} = \sigma a_2 \sin(\omega_0 t - \alpha)$, and $[\hat{u}_x \hat{v}_y - \hat{u}_y \hat{v}_x]_{\text{tip}} = -\sigma a_1 a_2 \sin(\alpha - \beta)$. a_1, a_2, α , and β are four coefficients. Comparing Eq. (1) with Eq. (2), one can see that $\Gamma_1 = ME_x u_x + ME_y u_y$ and $\Gamma_2 = 0$, then we get an approximate formula for the drift velocity:

$$V_x = -0.5ME_x + 0.5ME_x \csc(\alpha - \beta) \sin(2\omega_0 t - \beta - \alpha) + 0.5ME_y \sigma \cot(\alpha - \beta) - 0.5ME_y \sigma \csc(\alpha - \beta) \cos(2\omega_0 t - \beta - \alpha), \quad (3)$$

$$V_y = -\sigma 0.5ME_x \cot(\alpha - \beta) - \sigma 0.5ME_x \times \csc(\alpha - \beta) \cos(2\omega_0 t - \beta - \alpha) - 0.5ME_y - 0.5ME_y \times \csc(\alpha - \beta) \sin(2\omega_0 t - \beta - \alpha).$$

A clear conclusion in Eq. (3) is that the spiral wave undergoes a directional drift only when the electric-field frequency is zero or twice the spiral frequency.

When a dc electric field is applied, only the components that do not include time contribute to the constant drift of the spiral tip:

$$\bar{V}_x = -0.5ME_0 + \sigma 0.5ME_0 \cot(\alpha - \beta),$$

$$\bar{V}_y = -0.5ME_0 - \sigma 0.5ME_0 \cot(\alpha - \beta)$$

and

$$\bar{V}_d = \sqrt{\bar{V}_x^2 + \bar{V}_y^2} = \frac{\sqrt{2}}{2} ME_0 |\csc(\beta - \alpha)| = 0.5ME_d |\csc(\beta - \alpha)|. \quad (4)$$

It shows that the drift speed is proportional to the amplitude of the weak dc electric field E_d , which agrees with the numerical results in Fig. 4.

The application of a polarized electric field with $\omega = 2\omega_0$ will induce the spiral to drift with the velocity:

$$\bar{V}_x = 0.25ME_0 \csc(\beta - \alpha) [\sigma \cos(\beta + \alpha + \phi_2) + \sin(\beta + \alpha + \phi_1)], \quad (5)$$

$$\bar{V}_y = 0.25ME_0 \csc(\beta - \alpha) [\sigma \cos(\beta + \alpha + \phi_1) - \sin(\beta + \alpha + \phi_2)],$$

and the drift speed

$$\bar{V}_a = \sqrt{\bar{V}_x^2 + \bar{V}_y^2} = \sqrt{2/4}ME_0 |\csc(\beta - \alpha)| \sqrt{1 - \sigma \sin \phi}. \quad (6)$$

From this relation, we can see that the drift speed is determined by the phase difference ϕ besides other settled parameters. When $\phi = 2K\pi + 3\pi/2$ (for $\sigma = 1$) or $2K\pi + \pi/2$ (for $\sigma = -1$), the spiral drifts with the maximal speed. The drift velocity vanishes once ϕ is equal to either $2K\pi + \pi/2$ ($\sigma = 1$) or $2K\pi + 3\pi/2$ ($\sigma = -1$). Let the numerical result of the drift speed value at phase difference π be equal to \bar{V}_a according to (6) and we can get the value of $|\csc(\beta - \alpha)|$. Note that we also get almost the same value of $|\csc(\beta - \alpha)|$ from Eq. (4) and the numerical results in Fig. 4. Consequently, we can get the theoretical drift speed values at other phase differences ϕ from (6). The theoretical values are shown in Fig. 3(a), which are consistent with the numerical results.

From relation (5) one can give the drift angle dependence:

$$\tan \Theta = \frac{\bar{V}_y}{\bar{V}_x} = \begin{cases} \tan\left(-\frac{\phi_1 + \phi_2}{2} - \beta - \alpha + \frac{\pi}{4}\right), & \sigma = 1 \\ \tan\left(\frac{\phi_1 + \phi_2}{2} + \beta + \alpha + \frac{\pi}{4}\right), & \sigma = -1. \end{cases} \quad (7)$$

It indicates that it is the sum value of phase ($\phi_1 + \phi_2$) that determines the drift angle, not the phase difference ($\phi_2 - \phi_1$). From Eq. (7), we can also get $\Theta_{\sigma=1} + \Theta_{\sigma=-1} = k\pi + \pi/2$, which agrees well with the numerical results in Fig. 3(b).

In summary, the resonant drift behavior of spiral waves under a polarized electric field is studied in detail. Since both the spiral and polarized electric field have a characteristic of rotation symmetry, some interesting drift phenomena of the spiral induced by rotating polarized electric fields are observed. The system resonates at a frequency $\omega = 2\omega_0$ and thus the spiral tip drifts in a straight line. When the electric field is circularly polarized and its rotation follows that of the spiral wave, the spiral drifts the fastest; when the polarized electric field rotates contrary to that of the spiral, the spiral does not drift. The drift velocity can be controlled by changing the phase difference of the imposed polarized electric field. All simulation results are qualitatively consistent with our theoretical analysis based on the weak deformation approximation. Since electric fields in one direction have been em-

ployed to investigate the drift behavior of spiral waves in the BZ reaction,^{19,20,22,28} we hope that our theoretical results of the spiral drift controlled by a polarized electric field will be observed in experiments, such as the BZ reaction. Besides the drift of spiral waves, we expect that other effects of the polarized electric field on spiral waves as well as Turing patterns in chemical reaction-diffusion systems will be studied in the future.

This work was supported by the National Natural Science Foundation of China (Nos. 10405020 and 10225419) and the Start-Up Fund for Returned Overseas Chinese Scholars.

- ¹M. C. Cross and P. C. Hohenberg, *Rev. Mod. Phys.* **65**, 851 (1993).
- ²A. T. Winfree, *When Time Breaks Down* (Princeton University Press, Princeton, NJ, 1987).
- ³A. T. Winfree, *Science* **175**, 643 (1972).
- ⁴S. Jakubith, H. H. Rotermund, W. Engel, A. von Oertzen, and G. Ertl, *Phys. Rev. Lett.* **65**, 3013 (1990).
- ⁵F. Siegert and C. J. Weijer, *Physica D* **49**, 224 (1991).
- ⁶J. M. Davidenko, A. M. Pertsov, K. Salomonsz, W. T. Baxter, and J. Jalife, *Nature (London)* **355**, 349 (1991).
- ⁷A. T. Winfree, *Science* **266**, 1003 (1994); R. A. Gray, J. Jalife, A. V. Panfilov, W. T. Baxter, C. Cabo, J. M. Davidenko, and A. M. Pertsov, *ibid.* **270**, 1222 (1995); R. A. Gray, A. M. Pertsov, and J. Jalife, *Nature (London)* **392**, 75 (1998); F. X. Witkowski, L. J. Leon, P. A. Penkoske, W. R. Giles, M. L. Spano, W. L. Ditto, and A. T. Winfree, *ibid.* **392**, 78 (1998). For reviews, see Focus Issue: Fibrillation in Normal Ventricular Myocardium, *Chaos* **8**, 1 (1998); Focus Issue: Mapping and Control of Complex Cardiac Arrhythmias, *ibid.* **12**, 3 (2002).
- ⁸S. Alonzo, F. Sagues, and A. S. Mikhailov, *Science* **299**, 1722 (2003); H. Zhang, Z. Cao, N.-J. Wu, H.-P. Ying, and G. Hu, *Phys. Rev. Lett.* **94**, 188301 (2005).
- ⁹K. I. Agladze, V. A. Davydov, and A. S. Mikhailov, *JETP Lett.* **45**, 767 (1987).
- ¹⁰V. Biktashev and A. Holden, *Chaos, Solitons Fractals* **5**, 575 (1995).
- ¹¹A. Schrader, M. Braune, and H. Engel, *Phys. Rev. E* **52**, 98 (1995).
- ¹²V. Zykov, O. Steinbock, and S. C. Muller, *Chaos* **4**, 509 (1994).
- ¹³S. Nettesheim, A. von Oertzen, H. Rotermund, and G. Ertl, *J. Chem. Phys.* **98**, 9977 (1993).
- ¹⁴A. Mikhailov, V. Davydov, and V. Zykov, *Physica D* **70**, 1 (1994).
- ¹⁵R. M. Mantel and D. Barkley, *Phys. Rev. E* **54**, 4791 (1996).
- ¹⁶I. V. Biktasheva and V. N. Biktashev, *Phys. Rev. E* **67**, 026221 (2003).
- ¹⁷H. Zhang, N. J. Wu, H. P. Ying, G. Hu, and B. Hu, *J. Chem. Phys.* **121**, 7276 (2004).
- ¹⁸A. P. Munuzuri, C. Innocenti, J.-M. Flesselles, J.-M. Gilli, K. I. Agladze, and V. I. Krinsky, *Phys. Rev. E* **50**, R667 (1994).
- ¹⁹O. Steinbock, J. Schutze, and S. C. Muller, *Phys. Rev. Lett.* **68**, 248 (1992).
- ²⁰K. I. Agladze and P. De Kepper, *J. Phys. Chem.* **96**, 5239 (1992).
- ²¹V. Krinsky, E. Hamm, and V. Voignier, *Phys. Rev. Lett.* **76**, 3854 (1996).
- ²²B. Schmidt and S. C. Muller, *Phys. Rev. E* **55**, 4390 (1997).
- ²³H. Henry and V. Hakim, *Phys. Rev. E* **65**, 046235 (2002).
- ²⁴A. P. Munuzuri, M. Gomez-Gesteira, V. Perez-Munuzuri, V. I. Krinsky, and V. Perez-Villar, *Phys. Rev. E* **48**, R3232 (1993).
- ²⁵V. Voignier, E. Hamm, and V. Krinsky, *Chaos* **9**, 238 (1999).
- ²⁶M. Wellner, A. M. Pertsov, and J. Jalife, *Phys. Rev. E* **59**, 5192 (1999).
- ²⁷H. Henry, *Phys. Rev. E* **70**, 026204 (2004).
- ²⁸A. P. Munuzuri, M. Gomez-Gesteira, V. Perez-Munuzuri, V. I. Krinsky, and V. Perez-Villar, *Phys. Rev. E* **50**, 4258 (1994).
- ²⁹H. Zhang, B. Hu, G. Hu, and J. Xiao, *J. Chem. Phys.* **119**, 4468 (2003).
- ³⁰M. Bar and M. Eiswirth, *Phys. Rev. E* **48**, R1635 (1993); M. Hildebrand, M. Bar, and M. Eiswirth, *Phys. Rev. Lett.* **75**, 1503 (1995).